Available online at www.sciencedirect.com

ScienceDirect

Procedia CIRP 87 (2020) 385–390

www.elsevier.com/locate/procedia

5th CIRP CSI 2020

3D FIB/FESEM tomography of grinding-induced damage in WC-Co cemented carbides

J. Yang[1,2,3], J.J Roa[1,4], M. Odén[2], M.P. Johansson-Jõesaar[2,5] and L. Llanes[1,4]*

[1] CIEFMA – Department of Materials Science and Engineering, EEBE, Universitat Politècnica de Catalunya – BarcelonaTech, Barcelona 08019, Spain
[2] Nanostructured Materials, Department of Physics, Chemistry, and Biology (IFM), Linköping University, Linköping 58183, Sweden
[3] AMES-Sintered Metallic Components, Barcelona 08620, Spain
[4] Barcelona Research Center in Multiscale Science and Engineering, Universitat Politècnica de Catalunya, Barcelona 08019, Spain
[5] SECO Tools AB, Fagersta 73782, Sweden

* Corresponding author, *E-mail address:* luis.miguel.llanes@upc.edu

Abstract

WC-Co cemented carbides (hardmetals) represent the backbone materials for the tooling industry. In order to achieve particular tool geometries, diamond wheel grinding is a well-established method for machining hardmetals. Grinding-induced damage has been proven to strongly affect the performance and reliability of the machined tools. Assessment of grinding-mechanisms and induced surface integrity changes has usually been limited to monolithic ceramics, and it is particularly done on the basis of post-failure fractographic examination. In this work, characterization of grinding-induced damage of a WC-Co grade has been conducted by means of focused ion beam (FIB) tomography. The study includes a 3D description of the damage scenario, based on a reconstruction from successive parallel slices. Our results show that grinding induces a 200-400 nm thick surface layer containing fragmented WC grains and smeared Co phase morphology. A highly anisotropic subsurface microcrack network is generated. The discerned microcracks follow different microstructural paths: running through the binder, close to WC/Co interfaces or transgranular within the carbide phase. Very interesting, completely or near- lateral cracks (parallel to the ground surface) are found to be the predominant damage feature, whereas only few completely or near- orthogonal (perpendicular to the ground surface) cracks are discerned. Results are discussed in terms of material removal mechanisms during grinding of cemented carbides and surface integrity effects on the mechanical performance of hardmetal tools under service conditions.

© 2020 The Authors. Published by Elsevier B.V.
This is an open access article under the CC BY-NC-ND license (http://creativecommons.org/licenses/by-nc-nd/4.0/)
Peer-review under responsibility of the scientific committee of the 5th CIRP CSI 2020

Keywords: Cemented Carbides; Grinding; Microcracking; FIB; 3D tomography

1.Introduction

Cemented carbides are essentially ceramic-metal composites consisting of hard refractory carbides sintered together with tough iron group metals. These two distinct constituents yield them an excellent combination of mechanical properties (hardness, strength and toughness) and unique abrasion/wear resistance. Accordingly, cemented carbides are widely used as cutting/forming tools and structural components. The majority of the cemented carbides employed as cutting tools are WC-Co grades, often simply termed as hardmetals [1].

After being sintered, cemented carbides need to pass a manufacturing process to fulfill the requirements of the final tools [2,3]. Diamond grinding is a primary shaping process for these materials to achieve a particular tool geometry and/or close tolerances prescribed by its design. Similar to other hard/brittle materials [4], grinding of cemented carbides changes the surface integrity of the materials by inducing microcracks, residual stresses and/or phase transformation of the metallic binder (e.g. Refs. [3,5-9]. Surface integrity alterations play a crucial role in dictating the mechanical and tribological response of these ground materials, like fracture strength, fatigue and wear, etc. On the other hand, as grinding is a repetitive

2212-8271 © 2020 The Authors. Published by Elsevier B.V.
This is an open access article under the CC BY-NC-ND license (http://creativecommons.org/licenses/by-nc-nd/4.0/)
Peer-review under responsibility of the scientific committee of the 5th CIRP CSI 2020
10.1016/j.procir.2020.02.070

abrasion movement, investigation of how grinding affects the surface/subsurface of the materials provides more insights in understanding tribological behavior (scratch and/or wear, etc.).

The fact that grinding induces damage in hard and brittle materials is known. In this regard, extensive research conducted on fracture origins in single crystal and polycrystalline ceramics points out the existence of a dual population of cracks, oriented approximately perpendicular and parallel, respectively, to the grinding direction [4,10]. This anisotropy in terms of damage can result in quite distinct strength values, as a ground workpiece is stressed in various directions. However, literature information about the nature and distribution of grinding-induced microcracks in cemented carbides is scarce. Hegeman et al. [6] applied fractured cross-section analysis and found a deformed layer consisting of fragmented and pulverized grains and smeared out cobalt on top of the ground surface.

Over the past years, focused ion beam combined with field-emission scanning electron microscope (FIB/FESEM) systems have emerged as a useful advanced technique for characterizing microstructure, surface modification and deformation/damage in a wide range of materials [11,12]. In the case of cemented carbides, it has been successfully implemented for quantifying microstructure, evaluating tribological and mechanical phenomena, and assessing fatigue crack growth and corrosion behavior [13-21].

Grinding-induced damage in WC-Co using cross section view by FIB milling has been previously reported [8,9,22,23]. However, detailed information about crack distribution and microstructure-damage interaction cannot be captured from inspection of single cross-sections. On the other hand, FIB has recently shown to be a suitable technique for three-dimensional (3D) image reconstruction of small-scale scenarios [17,19,20].

This is related to its ability to perform site-specific and sequential SEM cross-sections. Compared to other conventional sectioning methods, based on the use of X-rays, transmission electron microscope (TEM) and/or atom probe tomography, FIB-base protocols require little or no specimen preparation, and is readily applicable to a wide range of materials. Moreover, it can be combined with other characterization techniques, such as energy dispersive x-ray spectroscopy or electron back scattered diffraction, to provide chemical and crystallographic data in 3D [24].

This study aims to implement FIB tomography, i.e. sequential FIB milling and subsequent FESEM imaging steps followed by an overall 3D reconstruction and visualization, for evaluation of subsurface grind-related damages. Special attention was paid to the distribution and orientation of the induced cracks as well as the corresponding microstructure-damage interaction.

2. Experimental Procedure

The hardmetal studied in this work is a WC- 13 wt.% Co grade with a carbide mean grain size of 0.7 μm. Grades with submicron (and finer) carbide size and binder content between 6 and 15% in weight are the most common hardmetal inserts used in the cutting tool industry, because they exhibit high hardness and toughness, combined with elevated compressive and edge strength together with superior abrasive resistance [1]. Vickers hardness and fracture toughness for the material here studied have previously been assessed as 14.8 GPa and 11.2 MPa√m, respectively [25]. Shaping of the cutting tool inserts was performed with an industrial plane surface grinding protocol at SECO Tools AB, making use of a commercial diamond abrasive wheel in combination with a coolant to reduce the heat generated.

Grinding-induced subsurface features were viewed using a FIB/FESEM dual beam Zeiss Neon 40 work station. The focused ion beam was used for sequential milling, while 2D x-y serial sections images were recorded using an electron beam (Fig. 1a). Before ion milling, a platinum layer was deposited on the region of interest to prevent re-deposition, erosion and curtain effects during milling (Fig. 1b). A frontal trench was opened using the ion beam for generating a cross-sectional surface (normal incidence to were identified and traced in each 2D image. Then, based on the batches of serial images, a 3D reconstruction of the damage scenario was obtained, using commercial Avizo software. Image processing consisted of different steps: image alignment, implementation of several filters to

improve image quality as well as to differentiate the three regions (WC, Co, and cracks), and final assignment of specific colors to each phase.

It should be noted here that real reconstructed volume is smaller than the total FIB-milled one. It is mainly due to the fact that artificial effects during FIB milling such as waterfall/material resputtered may cover part of the milled cross-section surface (imaged at 45000X).

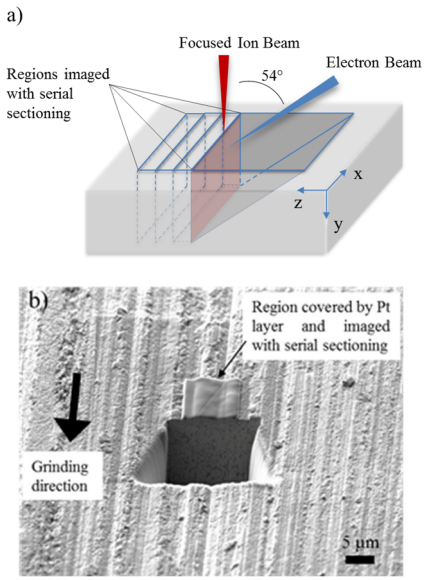

Fig. 1 (a) Schematic of FIB serial sectioning process; and (b) SEM image of frontal trench opened by FIB. Note that Pt deposited square area is the region being serial sectioned later. Grinding direction is marked by a white arrow.

3. Results and Discussion

3.1 Surface topography

Grinding is commonly used as a primary choice for machining hardmetal tools. A grinding wheel containing diamond grits with sharp edges embedded in a softer binder is rotated against the material surface. Simultaneously, coolant is applied for minimizing the heat effect. The material removal mechanism is an intensive abrasive process affecting both WC and Co phases. Carbide grains are either cracked by the tensile stresses induced by the abrasive particles or plastically deformed by the compressive stresses in front of them. On the other hand, Co phase is smeared out from the surface with pulverized WC particles, and partly removed together with the WC fragments [6]. Consequently, the surface topography was modified by the grinding process. A surface texture can be discerned in Fig.1b with an unidirectional groove-like feature originating from the relative movement of the grinding wheel with respect to the hardmetal surface (see white arrow). This kind of anisotropy texture is suggested to have an effect on tribomechanical response of the material. Meanwhile, the geometrical discontinuities such as peaks and valleys exist as stress concentrators compared to flat surface [26].

3.2 3D FIB tomography of subsurface cracks

Grinding induces subsurface damage to the material and the resulting 3D network of the cracks is complex, particularly in the composite material studied. FIB tomography is then applied here for the first time for quantitative analysis of 3D grinding-induced crack networks in hardmetals.

3.2.1 Subsurface features: 2D analysis

Fig. 2 shows a series of representative cross-sectional images. It should be noticed that grinding direction is orthogonal to the screen in this configuration. Several observations may be highlighted from inspection of these 2D images. First, grinding damage is localized within a surface layer of approximately 200-400 nm in thickness, containing pulverized WC grains and smeared Co phase. This observation is in good agreement with those reported by Zuñega et al. [27]. In that study, as a consequence of multi-scratch testing using a diamond indenter, a tribo-layer composed of fragmented nano-sized WC grains embedded in a Co metallic matrix was generated. Such tribolayer was reported by them as a completely novel finding, speculated to exist as a possible protective layer or self-healing mechanism for the WC-Co hardmetals when abraded at very low speeds at room temperature. The protective and/or self-healing description was coined, because it seemed to be helpful in arresting further extension of the discerned damage into the bulk material underneath the tribolayer [27]. Second, microcracking was identified to follow different microstructural paths: either

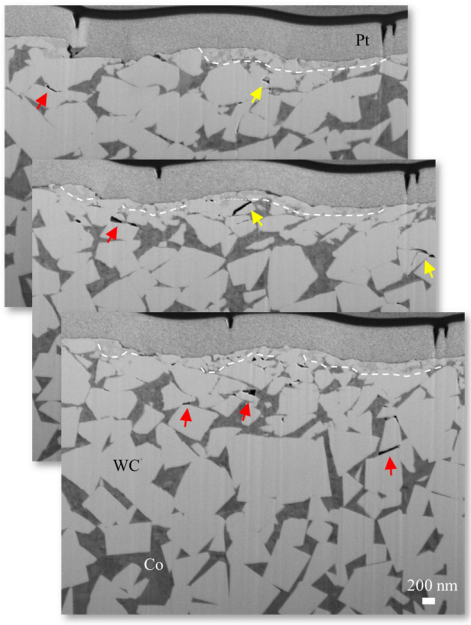

Fig. 2 Representative examples of multiple parallel 2D FIB cross-sections, showing the evidenced subsurface damage. The viewing angle is 36° from the milled plane. Cracks following either WC/Co interface or transgranular paths are indicated by red and yellow arrows respectively. The surface layer containing fragmented WC grains and smeared Co phase is differentiated from the underneath bulk material by dashed white lines.

running through the binder or at WC/Co interfaces (red arrows), or transgranular within the carbide phase (yellow arrows), the former being more predominant than the latter. Similar findings to those identified after grinding have been reported under abrasive wear in previous studies. For instance, Larsen-Basse et al. [28] did a systematic microscopic examination of rock drilling WC-Co tool bits, and pointed out that abrasive wear occurs by preferential removal of the cobalt metal binder between the WC grains, followed by carbide spalling mainly through intergranular fracture. Third, close inspection of the subsurface, just beneath the referred tribolayer, reveals severe plastic deformation within binder phase. It is evidenced by the pronounced image contrast at length scales smaller than the binder thickness between the carbide grains. Co experiences noticeable metallurgical changes, and detailed information – as gathered through electron back-scattered diffraction and TEM analysis – may be found in a recently published work by the authors [9].

3.2.2 Grinding-induced crack distribution network: 3D view

Fig. 3 presents the 3D reconstruction of the microcracking network. It is shown from two different view perspectives, depending on the orientation of grinding direction with respect to the screen: perpendicular (Fig. 3a), and inclined at some degree (Fig. 3b). A schematic diagram of the cracking features observed at the subsurface level is outlined in Fig. 3c, to illustrate some relevant aspects. Reference points, regarding different grinding-groove peaks/valleys, are also identified in Fig. 3. Surface region examined contains two grooves. Reference points B and D represent the bottom of the two residual grinding grooves, whereas A, C and E correspond to the groove edges, where some material is piled-up. Note that the tribolayer discerned in the 2D images is not sketched in Fig. 3c.

Analysis of 3D reconstruction together with implementation of the material statistic module in the Avizo software allows to quantify different parameters related to the microcracking scenario. On one hand, shape and distribution of the microcracks, the latter in terms of orientation with respect to grinding direction, may be assessed. On the other hand, volume fraction and geometry dimensions of microcracks may also be measured. These findings can be summarized as: first, although the grinding-induced microcracking network is complex, it is evidenced to be highly anisotropic. In this regard, most of the cracks observed are completely or near- lateral ones, parallel to the ground surface. Meanwhile, only few median (longitudinal) or radial (transversal) cracks running completely or near- orthogonal to the ground surface (i.e. following symmetry median planes containing the load axis of abrasive particles) are seen. Second, the relative volumetric content of the “phases” considered: WC, Co and cracks (as quantified by means of module within Avizo software) yield values of 80.5, 19.4 and 0.1 vol.%, respectively. The binder-related value is comparable with the theoretical volume percentage of Co phase (i.e. 21 vol.%). Third, the highest frequent length of the discerned cracks is 28 nm, and over 90% of them exhibit a length within the range of 5 to 60 nm.

The anisotropic cracking network here evidenced should be a direct result of the plastic/elastic deformation and the strain mismatch inside the bulk matrix. Studies carried on static indentation, scratch and grinding of monolithic ceramics have reported that median/radial cracks initiate from flaws at the deformation boundary and are driven by the residual stress field arising from strain mismatch between plastically and elastically deformed regions [4,10,29]. Within this context, the role played by the phase assemblage of hardmetals: two-phase interpenetrating networks with quite distinct individual properties, should be invoked for analyzing the discerned cracking scenario. On one hand, the ductile nature of the Co binder phase may be speculated to impede stress concentrators and crack nucleation. Furthermore, it may yield a more gradual residual stress field evolution; and thus, a less pronounced strain mismatch between the plastically deformed zone and the surrounding elastically restraining matrix. Under these conditions, nucleation and extension of median/radial cracks would be partly suppressed or even inhibited. On the other hand, random distribution of carbides may also translate into more effective obstacles, since median crack initiation and growth need to cross intragranular paths too.

From a practical viewpoint, the anisotropic nature of the microcracking network must be assessed as beneficial for effective machining of cemented carbides. In this regard, the correlation between prominence of lateral crack and more material removal would point out that spalling-like failure micromechanism exhibited by the hardmetal studied implies a relatively lower energy consumption during the grinding process. Beneficial description may also be recalled from a mechanical integrity viewpoint, as lower frequency of median cracks results in less pronounced effects regarding strength lessening, when the ground material is subjected to external stresses under service conditions.

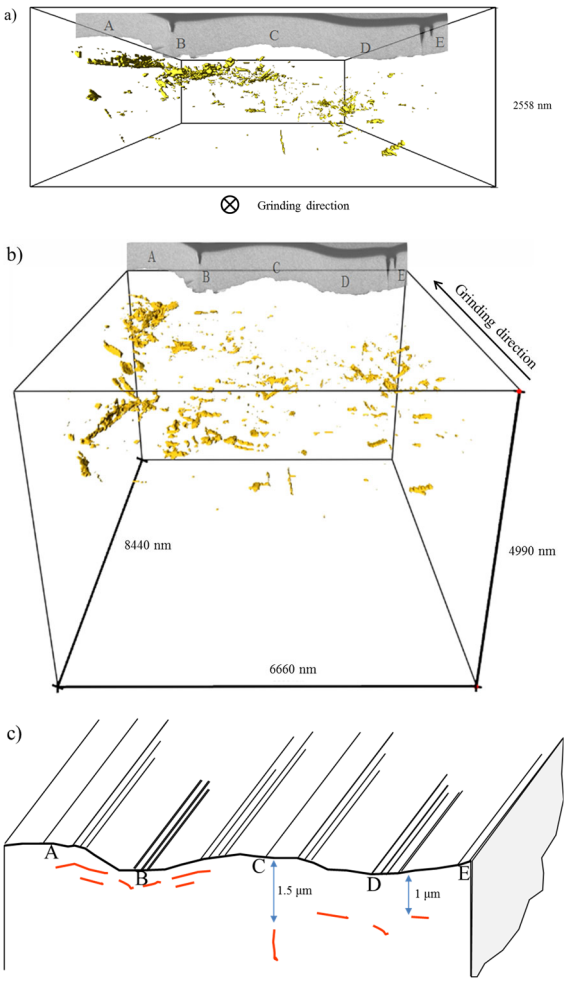

Fig. 3 3D reconstruction of the microcrack network, within the interpreted volume. It is shown from two different view perspectives depending on the orientation of grinding direction with respect to the screen: perpendicular (a), and inclined some degree (b). The dimension of the interpreted region is listed. A schematic diagram of subsurface crack types, observed beneath ground surface, are given in (c). Note that here cracks are indicated by red segments. Labels (A)–(E) denote surface region discussed in the text.

4. Summary

3D FIB/FESEM tomography has been successfully implemented for visualizing and characterizing the microcracking network induced by grinding of a WC-Co hardmetal grade. The existence of a thin surface layer containing pulverized WC grains and smeared Co phase is confirmed. Just below it, a complex microcracking network is discerned. The observed microcracks follow different microstructural paths: running through either binder or carbides, or following WC/Co interfaces. The most relevant finding is the highly anisotropic character of the microcrack distribution. In this regard, completely or

near- lateral cracks (parallel to the ground surface) are found to be the predominant damage feature, whereas only few completely or near- orthogonal (perpendicular to the ground surface) cracks are discerned. It is suggested to be related to the strain mismatch inside the bulk matrix as well as the strain interaction between the two different and interpenetrated constitutive phases.

Acknowledgements

Funding for this investigation was partly supplied by the Spanish MICINN - FEDER (Grant No. PGC2018-096855-B-C41). One of the authors (J.Y.) acknowledges funding received through Erasmus Mundus joint European Doctoral Programme DocMASE. Research work was conducted within a cooperative effort among SECO Tools AB, Linköping University and Universitat Politècnica de Catalunya.

References

[1] Prakash L. 1.02 - Fundamentals and General Applications of Hardmetals. In: Sarin VK, Mari D, Llanes L (Eds.) Comprehensive Hard Materials. Oxford: Elsevier; 2014. Vol. 1, p. 29-90.
[2] Byrne G, Dornfeld D, Denkena B. Advancing cutting technology. CIRP Ann-Manuf Techn. 2003;52:483-507.
[3] Breidenstein B, Denkena B. Significance of residual stress in PVD-coated carbide cutting tools. CIRP Ann-Manuf Techn. 2013;62:67-70.
[4] Li K, Warren Liao T. Surface/subsurface damage and the fracture strength of ground ceramics. J Mater Process Technol. 1996;57:207-20.
[5] Tönshoff HK, Karpuschewski B, Mohlfeld A, Seegers H. Influence of subsurface properties on the adhesion strength of sputtered hard coatings. Surf Coat Tech. 1999;116–119:524-9.
[6] Hegeman JBJW, De Hosson JTM, de With G. Grinding of WC–Co hardmetals. Wear. 2001;248:187-96.
[7] Yang J, Odén M, Johansson-Jõesaar MP, Llanes L. Grinding effects on surface integrity and mechanical strength of WC-Co cemented carbides. Procedia CIRP. 2014;13:257-63.
[8] Yang J, Odén M, Johansson-Jõesaar MP, Esteve J, Llanes L, Mechanical strength of ground WC-Co cemented carbides after coating deposition. Mater Sci Eng A. 2017;689:72-7.
[9] Yang J, Roa JJ, Schwind M, Odén M, Johansson-Jõesaar MP, Llanes L, Grinding-induced metallurgical alterations in the binder phase of WC-Co cemented carbides. Mater Charact 2017;134:302-10.
[10] Subhash G, Marszalek MA, Maiti S. Sensitivity of scratch resistance to grinding-induced damage anisotropy in silicon nitride. J Am Ceram Soc. 2006;89:2528-36.
[11] Phaneuf MW. Applications of focused ion beam microscopy to materials science specimens. Micron. 1999;30:277-88.
[12] Munroe PR. The application of focused ion beam microscopy in the material sciences. Mater Charact. 2009;60:2-13.
[13] Cairney JM, Munroe PR, Schneibel JH. Examination of fracture surfaces using focused ion beam milling. Scr Mater. 2000;42:473-8.
[14] Beste U, Coronel E, Jacobson S. Wear induced material modifications of cemented carbide rock drill buttons. Int J Refract Met Hard Mater. 2006;24:168-76.
[15] Gant AJ, Gee MG, Gohil DD, Jones HG, Orkney LP. Use of FIB/SEM to assess the tribo-corrosion of WC/Co hardmetals in model single point abrasion experiments. Tribol Int. 2013;68:56-66.
[16] Tarragó JM, Jimenez-Piqué E, Schneider L, Casellas D, Torres Y, Llanes L. FIB/FESEM experimental and analytical assessment of R-curve behavior of WC–Co cemented carbides. Mater Sci Eng A. 2015;645:142-9.
[17] Tarragó JM, Fargas G, Isern L, Dorvlo S, Tarrés E, Müller CM, Jimenez-Piqué E, Llanes L. Microstructural influence on tolerance to corrosion-induced damage in hardmetals . Mater Design. 2016;111:36-43.
[18] Jones HG, Norgren SM, Kritikos M, Mingard KP, Gee MG. Examination of wear damage to rock-mining hardmetal drill bits. Int J Refract Met Hard Mater. 2017;66:1-10.
[19] Jimenez-Piqué E, Turon-Vinas M, Chen H, Trifonov T, Fair J, Tarrés E, Llanes L. Focused ion beam tomography of WC-Co cemented carbides. Int J Refract Met Hard Mater. 2017;67:9-17.
[20] Mingard KP, Roebuck B, Jones HG, Stewart M, Cox D, Gee MG. Visualisation and measurement of hardmetal microstructures in 3D. Int J Refract Met Hard Mater. 2018;71:285-91.
[21] Llanes L. In-depth understanding of fatigue micromechanisms in cemented carbides: Implications for optimal microstructural tailoring. Metals 2019;9:924.
[22] Yang J, Roa JJ, Odén M, Johansson-Jõesaar MP, Esteve J, Llanes L. Substrate surface finish effects on scratch resistance and failure mechanisms of TiN-coated hardmetals. Surf Coat Tech. 2015;265:174-84.
[23] Yang J, García Marro F, Trifonov T, Odén M, Johansson-Jõesaar MP, Llanes L. Contact damage resistance of TiN-coated hardmetals: Beneficial effects associated with substrate grinding. Surf Coat Tech. 2015;275:133-41.
[24] Borgh I, Hedström P, Odqvist J, Borgenstam A, Ågren J, Gholinia A, Winiarski B, Withers PJ, Thompson GE, Mingard K, Gee MG. On the three-dimensional structure of WC grains in cemented carbides. Acta Metall. 2013;61:4726-33.
[25] Sheikh S, M'Saoubi R, Flasar P, Schwind M, Persson T, Yang J, Llanes L. Fracture toughness of cemented carbides: Testing method and microstructural effects. Int J Refract Met Hard Mater. 2015;49:153-60.
[26] Evans AG, Crumley GB, Demaray RE. On the mechanical behavior of brittle coatings and layers. Oxid Met. 1983;20:193-216.
[27] Zuñega JCP, Gee MG, Wood RJK, Walker J. Scratch testing of WC/Co hardmetals. Tribol Int. 2012;54:77-86.
[28] Larsen-Basse J, Perrott CM, Robinson PM. Abrasive wear of tungsten carbide—cobalt composites. I. Rotary drilling tests. Mater Sci Eng. 1974;13:83-91.
[29] Lawn B, Evans AG, Marshall DB. Elastic/plastic indentation damage in ceramics: The median/radial crack system. J Am Ceram Soc. 1980;63:574-81.

2212-8271 © 2020 The Authors. Published by Elsevier B.V.
This is an open access article under the CC BY-NC-ND license (http://creativecommons.org/licenses/by-nc-nd/4.0/)
Peer-review under responsibility of the scientific committee of the 5th CIRP CSI 2020